American Mineralogist, Volume 84, pages 152–159, 1999

TEM investigation of Lewiston, Idaho, fibrolite: Microstructure and grain boundary energetics

R. Lee Penn,[1,*] Jillian F. Banfield,[2] and Derrill M. Kerrick[3]

[1]Materials Science Program, University of Wisconsin-Madison, Madison, Wisconsin 53706, U.S.A.
[2]Department of Geology and Geophysics, University of Wisconsin-Madison, Madison, Wisconsin 53706, U.S.A.
[3]Department of Geosciences, Pennsylvania State University, University Park, Pennsylvania 16802, U.S.A.

Abstract

High-resolution transmission electron microscopy (HRTEM) revealed that a sample of fine-grained Lewiston, Idaho, fibrolite is predominantly fibrolite with trace amounts of poorly crystalline layer silicates. The fibrolite consists of aggregates of acicular grains where the *c* axis of each grain is parallel to the elongation direction. Widths of 195 grains were measured: The average is 0.41 μm, the mode is 0.29 μm, and the range is 0.05–1.57 μm. No stacking faults or other extended defects were observed in any of the grains. Grain boundary energies were calculated using the symmetrical dislocation tilt wall theory (SDTW) and measurements of misorientation between the *c* axes of neighboring fibrolite crystals. The angles of misorientation range from 1° to 11°, yielding grain boundary energies ranging from 310 to 967 ergs/cm^2, respectively, with an average energy of 610 ergs/cm^2. Modeling the fibrolite grains as infinitely long cylinders and using the experimentally measured average grain diameter, an average molar grain boundary energy of 320 J/mol was calculated. This excess grain boundary energy could correspond to a shift of as much as +140 °C in the andalusite-sillimanite boundary and +30 °C in the kyanite-sillimanite boundary. Typical fibrolite grain boundaries adopt relatively high-energy configurations. We attribute this to fibrolite nucleation at pre-existing low-angle grain boundaries in layer silicates, preserving misorientations, and conferring a fine-grained texture.

Introduction

Phase relations in most coarse-grained rocks are well understood. However, when crystal size is small, a significant portion of the volume of material is comprised of grain boundaries or surfaces. Atoms with unsatisfied and distorted coordination environments are a source of excess energy and thus can significantly perturb mineral stability fields and phase transformation kinetics (Goldstein et al. 1992). The particle size dependence of stability fields is most important where the structure energies of polymorphs are similar. In some systems (e.g., Fe-oxides, Langmuir and Whittemore 1971; CdS, Goldstein et al. 1992; Ti-oxides, Gribb and Banfield 1997; Al-oxides, McHale et al. 1997) ''metastable'' compounds can become stable as particle size is reduced, leading to particle-size dependent stability fields (Zhang and Banfield, unpublished manuscript).

The aluminosilicate (Al_2SiO_5) polymorphs (kyanite, andalusite, and sillimanite) are common metamorphic minerals. Fibrolite is the fine-grained acicular habit of sillimanite that is common in medium- to high-grade metapelitic rocks. Aluminosilicates are extremely important in petrologic studies because the aluminosilicate phase relations are generally believed to be well understood and are used to obtain pressure and temperature information for metapelitic rocks. Because micro-scale features such as disorder, small grain size, defects, and compositional variation can be indicators of higher energy (or non-equilibrium) conditions, microstructural characterization of phases is essential for the determination of thermobarometric histories.

Univariant reactions in the kyanite-andalusite-sillimanite system involve reconstructive phase transformations that change the coordination number of aluminum and the connectivity of the silicate tetrahedra. These reactions are sluggish because they require rupture of strong Al-O and Si-O bonds and the driving forces are small. Consequently, small errors in experimental determinations of the univariant equilibria result in substantial uncertainty in the phase boundaries and thus, the location of the triple point. Furthermore, fine grain size, small amounts of impurities, or compositional variation, in addition to any structural and microstructural factors that modify the total energy of the aluminosilicate phases, can significantly modify the positions of the stability fields for kyanite, andalusite, and sillimanite.

Over the past two decades, considerable effort has been expended to identify factors that affect the energetics of the aluminosilicate phases. Dislocation density, cation substitution, aluminum-silicon disorder, non-stoichiome-

* E-mail: rlee@geology.wisc.edu

0003–004X/99/0102–0152$05.00

try, grain boundary area, and crystallographic mismatch between adjacent grains have been suggested as factors that modify phase stability (Helgeson 1978; Kerrick 1986; Holdaway and Mukhopadhyay 1993). Comparisons of thermodynamic studies designed to determine the energetic differences between fibrolite and coarse-grained sillimanite yield conflicting results. Experimental hydrothermal studies of Richardson et al. (1968), which examined the extent of reaction between phases at various temperatures and pressures, used a sillimanite/fibrolite sample (Brandywine Springs, Delaware) that was about 30 vol% fibrolite, whereas those of Newton (1966, 1969) used fibrolite-free sillimanite (Lichtfield, Connecticut). Their results were in relatively good agreement, suggesting that the presence of fibrolite does not shift the Al_2SiO_5 equilibrium boundaries (Kerrick 1990). However, in an investigation of the andalusite-sillimanite phase boundary, Holdaway (1971) performed hydrothermal experiments using andalusite (Minas Gerais, Brazil) and sillimanite (Benson Mines, New York or Montville Quadrangle, Connecticut) in one vessel and andalusite, sillimanite, and fibrolite (a mixture from Williamston, Australia or Jefferson City, Colorado) in another. He observed early reaction of fibrolite to andalusite, suggesting that fibrolite was less thermodynamically stable under the pressure and temperature conditions.

Anderson and Kleppa (1969) found measurable differences in the heats-of-solution of fibrolite (Custer, South Dakota) and sillimanite (Benson Mines, New York) using molten oxide calorimetry. Similarly, Salje (1986) found significant differences in the heat capacities of sillimanite (from Waldeck, Germany; Träskbole, Finland; and Sri Lanka) and fibrolite (Garcujuela, Spain), although those results are considered questionable due to insufficient sample size for the procedure used (Hemingway et al. 1991). In contrast, Hemingway et al. (1991) reported heat capacities for sillimanite (Sri Lanka) and fibrolite (Lewiston, Idaho) that were virtually identical at 298 K and differed by $<1\%$ at 1000 K. Topor's et al. (1989) mean measurements of the heat-of-solution of sillimanite (Sri Lanka) and fibrolite (Lewiston, Idaho) suggest that fibrolite has a slightly less negative heat-of-formation than sillimanite. However, the precision of the measurements preclude a definitive conclusion regarding the differences in the enthalpies of formation. Thus, although some experimental evidence suggests an energy difference between coarse-grained sillimanite and fibrolite, which would require different stability fields, the difference would probably be small and likely be masked by inherent uncertainty in experimental measurements.

In an alternative approach, Holdaway (1971) computed a molar surface energy for fibrolite of 351 ± 71 J/mol, assuming a square cross-section and grain diameters of about 0.3 μm, and using typical surface energies for silicates. This value corresponds to a temperature shift of about 120 °C from the sillimanite/andalusite equilibrium.

Although it is known how to calculate the free energy contribution to total energy due to grain size and angular mismatch between adjacent grains, no studies have conducted the grain boundary characterization necessary to model the energy of fibrolite compared to coarse sillimanite. Kerrick (1990) described a preliminary study by Wenk and Medrano where samples consisting of fibrolite aggregates were examined using electron diffraction to determine that the angular mismatch between neighboring grains of fibrolite was $<15°$. Based on that preliminary study, Kerrick (1990) used the symmetrical dislocation tilt wall (SDTW) theory to estimate the grain boundary contribution to the total free energy of fibrolite.

In this study, we measure the angular mismatch between adjacent fibrolite crystals and grain diameters, and use this information to estimate the grain boundary contribution to the total free energy using the SDTW theory for a fibrolite sample from Lewiston, Idaho. We also evaluate the importance of dislocation density and planar defects to the thermodynamic analysis, the layer silicate mineralogy, and the origin of the fibrolite grain boundary structure.

Experimental methods

Fibrolite from Lewiston, Idaho, has been extensively characterized, e.g., for calorimetry (Hemingway et al., unpublished manuscript; Topor et al. 1989), non-stoichiometry (Kerrick 1990; Hemingway et al. 1991), Al/Si disorder (Hemingway et al. 1991), and thermal expansion (Hemingway et al. 1991). Powders of fibrolite and coarse-grained sillimanite from Benson Mines, New York were examined using a Scintag PadV X-ray Powder Diffractometer.

Four 3 mm × 3 mm pieces of fibrolite were cut from two standard 30 μm thin sections, mechanically thinned, argon ion-milled to electron transparency, and examined using a Phillips CM20 ultra-twin 200 kV high-resolution transmission electron microscope (HRTEM) equipped with a GE twin window energy dispersive X-ray (EDX) and a NORAN voyager analyzer.

The degree of misorientation between adjacent crystals of fibrolite was determined using selected-area electron diffraction (SAED). Using the TEM sample holder tilting mechanisms, the sample was tilted until one grain was oriented with respect to the electron beam, and the tilts of the sample holder and the electron diffraction pattern recorded. The same procedure was repeated for the adjacent grain. The degree of misorientation between the three principle crystallographic directions was determined from the SAED patterns and sample tilt information using computer-based stereographic methods.

Results

Lattice parameter comparison

XRD examination of powders of fibrolite from Lewiston, Idaho, and coarse-grained sillimanite from Benson Mines, New York, revealed no significant differences in lattice parameters. A 50/50 mixture of the two materials showed no splitting of peaks. The full width at half max-

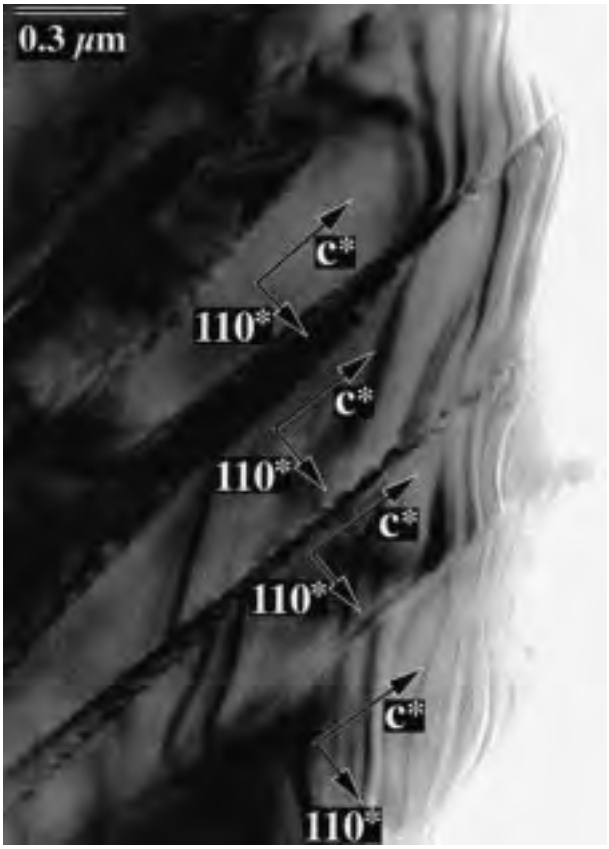

FIGURE 1. TEM micrograph showing a typical area of fibrolite from Lewiston, Idaho.

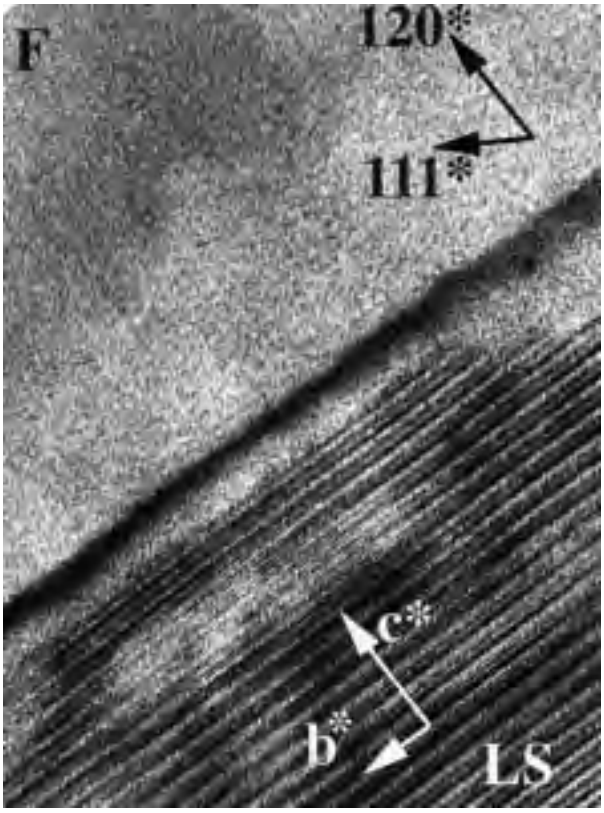

FIGURE 2. TEM micrograph of low-angle tilt boundary between a grain of fibrolite (F) and a grain of layer silicate (LS).

imum peak height and 2θ position of each peak were identical, within the standard error of the technique.

Mineralogy

Samples consisted of aggregates of acicular fibrolite grains, with their *c* axes parallel to the fiber axes, and approximately 1% layer silicates, present at grain boundaries. Figure 1 shows microstructure typical of Lewiston, Idaho, fibrolite. No quartz or corundum was observed in this sample.

The layer silicate mineralogy is complex. SAED patterns indicate that the basal spacing is ~1.0 nm. All [010] SAED patterns show a one-layer period in 20*l*, indicating that all are group A polytypes (Bailey 1988). The β angle varied considerably. Most commonly, β measured between and 95° and 100°. Streaking of 02*l* reflections indicates stacking is poorly ordered or disordered in roughly 10% of these crystals. Approximately 30% of crystals have ordered stacking with $\alpha = 90°$. This layer silicate is probably structurally related to $2M_1$ muscovite. EDX analyses indicate an Al-rich composition with interlayer Na, Ca, and some K (no Mg or Fe was detected). These dioctahedral layer silicates, which damage rapidly in the electron beam, are probably smectite. In about 50% of crystals, [100] SAED patterns indicate ordered stacking with a two-layer period and $\alpha \approx 85°$. The final 10% of layer silicates observed in this sample are characterized by ordered stacking characterized with one ($\alpha \neq 90°$) or four-layer ($\alpha = 90°$) periods in 02*l*. All layers silicates with $\alpha \neq 90°$ and the four-layer structure are non-standard polytypes.

Two predominant layer silicate morphologies were observed. In the first, the layer silicates are elongated perpendicular to [001] with the basal planes parallel to the elongation direction of the fibrolite. In this case, fibrolite crystals appear to have been partially or completely replaced by the layer silicate crystallizing along fibrolite grain boundaries (Fig. 2). The crystallographic relationship most commonly observed between this type of layer silicate crystal and fibrolite was $120^*_{\text{fibrolite}}$ approximately parallel to $c^*_{\text{layer silicate}}$ with the very small angular mismatch (0°–2°). In addition, $c^*_{\text{fibrolite}}$ approximately parallel to $c^*_{\text{layer silicate}}$ (0° to 15° mismatch) and $b^*_{\text{fibrolite}}$ approximately parallel to $c^*_{\text{layer silicate}}$ (0° to 15° mismatch) relationships were observed. In the second case, the layer silicates are tiny crystals bridging gaps between the corners or tips of adjacent fibrolite grains. Sheet silicates ranged in width from less than 0.1 μm to about 0.5 μm. The two-layer silicate morphologies have indistinguishable chemical compositions.

TABLE 1. Measured angles (in degrees) between principal directions in adjacent grains of Lewiston, Idaho fibrolite

Boundaries	Δa	Δb	Δc
P215-P217	1	1	1
P219-P221	2	2	2
P174-P179	2	3	2
P210-P212	3	2	2
P151-P154	1	3	3
P212-P215	2	4	2
P165-P170	2	5	3
P179-P181	5	4	4
P210-P203	4	6	1
P203-P204	6	5	1
P174-P175	5	5	5
P217-P219	7	5	3
P174-P181	3	6	7
P186-P187	7	7	3
P175-P181	8	3	8
P151-P159	8	8	3
P182-P185	9	9	2
P208-P209	12	6	11
P179-P182	15	15	2
P175-P178	20	20	2
P209-P210	18	17	8
P178-P186	48	48	4
P170-P171	49	18	43
P221-P222	53	53	11
P195-P198	45	52	31

Grain boundary and microstructure characterization

Table 1 lists the angular mismatch calculated for 25 grains. In 84% of the boundaries analyzed, the angular mismatch between the three principle crystallographic directions is <20°, with a mismatch between the *c* axes <12°. In 92% of the boundaries, the angular mismatch between neighboring *c* axes is <12°, and most are <6°. Figure 3 is an HRTEM image of a boundary where the angular mismatch between the *c* axes of neighboring grains is 1°. The absence of thickness or moiré fringes indicates that the boundary is nearly parallel to the electron beam direction. Based on the indexing of the electron diffraction patterns for each grain, the boundary plane is approximately parallel to (110).

Samples were examined with a petrographic microscope in order to estimate apparent average grain diameters. Crystals appeared to be at least a few micrometers in diameter. However, analysis of 20 TEM negatives reveal the actual average grain diameter to be 0.41 μm, the mode to be 0.29 μm, and the range to be 0.05–1.57 μm, as seen in Figure 4.

In the samples examined, dislocation densities are extremely low; in fact, in almost all cases, fibrolite crystals are essentially dislocation free ($\ll 10^8/cm^2$). No other extended defects were observed. Furthermore, SAED patterns show no evidence of streaking parallel to any direction, thereby suggesting little or no Al/Si disorder.

Modeling grain boundary energy using symmetrical dislocation tilt wall theory

Because the degree of angular mismatch between the *c* axes is typically <15°, the ''symmetrical dislocation tilt wall'' (SDTW) theory can be used to model the grain

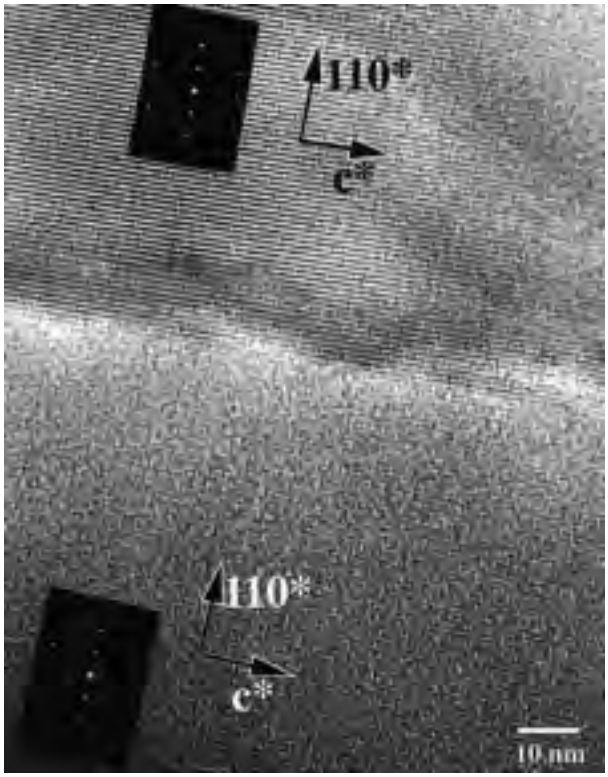

FIGURE 3. TEM micrograph of a low-angle grain boundary between two fibrolite crystallites where the degree of angular mismatch between the *c* axes is 1°. The zone axis SAED patterns are shown for each grain. In this image, the left-hand grain is oriented with respect to the electron beam.

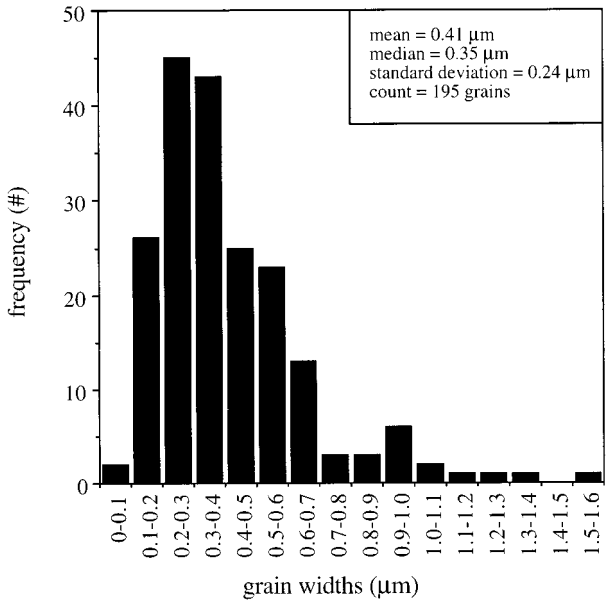

FIGURE 4. Grain widths of 195 fibrolite grains measured from 20 TEM micrographs.

FIGURE 5. TEM micrograph of a low-angle tilt boundary between two grains of fibrolite where the angle of mismatch between the *c* axes of each grain is 5°. Edge dislocations can clearly be seen if the image is viewed from a low angle.

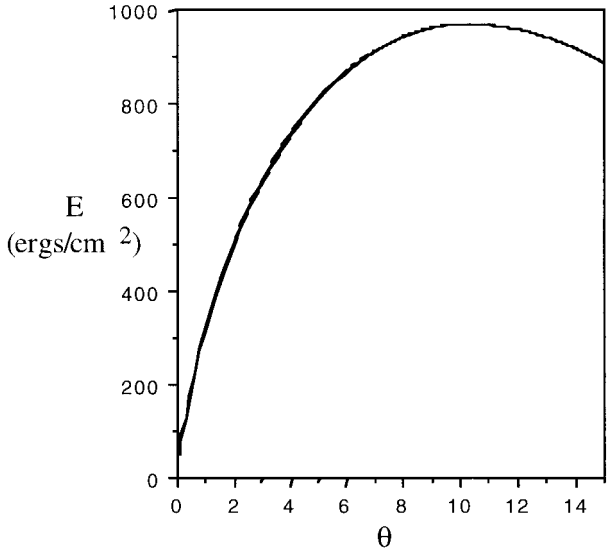

FIGURE 6. Dislocation tilt wall grain boundary energy as a function of angular mismatch, calculated using Equation 1.

boundary energy (Kerrick 1990). The advantage of SDTW is that no surface energy measurement is required because the energies of the grain boundaries are calculated from measured parameters (μ = shear modulus; θ = degree of angular mismatch). Symmetrical tilt walls are modeled as a series of parallel edge dislocations with the lattice structures of the grains symmetrically disposed about the boundary. These dislocations are clearly visible in Figure 5, where the angle of tilt at this boundary between the *c* axes of these two fibrolite crystals is about 5°. The plane containing the edge dislocations is the boundary between two symmetrically disposed crystals, and θ is the angle of misorientation between the two grains. The tilt wall energy (E_{TW}) as a function of angular misorientation is computed from:

$$E_{TW} = [\mu b/4\pi(1 - \nu)]\theta[\ln (b/r_o) - \ln \theta] \qquad (1)$$

where ν is Poisson's ratio. Values for ν and μ were both taken for sillimanite from Birch (1966) and Vaughan and Weidner (1978), respectively. In addition, assuming that $r_o = 2b$ (Kerrick, 1986) where *b* is the magnitude of the Burgers vector. By far the most common grain boundary orientation is approximately parallel to (110), with a Burgers vector of $d(110) = 0.53$ nm. Tilt wall energy vs. angular mismatch calculated from Equation 1 is shown in Figure 6. When θ is small, the $\theta\ln\theta$ term dominates, but when θ is large, the $\theta\ln(b/r_o)$ term dominates. Consequently, Equation 1 predicts a maximum computed grain boundary energy for an angular mismatch of about 10° (Kerrick 1990).

Because the SDTW approach models grain boundaries as a series of pure edge dislocations with the adjacent crystals symmetrically disposed about the boundary, it cannot accommodate asymmetry in the boundary. The *c* axis is parallel to the elongation direction, thus, usually lies in or is slightly inclined to the boundary between adjacent fibrolite grains. Consequently, in applying the SDTW model to estimate the grain boundary contribution to the total energy of Lewiston, Idaho, fibrolite, we chose to use the misorientation between the *c* axes of adjacent grains. This model does not account for the angular mismatch between the *a* and *b* crystallographic axes. However, using the angular mismatch between the other two axes does not result in a significantly different E_{TW}.

E_{TW} was calculated for each boundary. Results ranged from 310 to 970 ergs/cm^2. The average energy of the dislocation tilt wall boundaries characterized in this sample is 610 ergs/cm^2. The molar grain boundary area (*A*) was calculated using the experimentally obtained average diameters of fibrolite crystals reported in Figure 2. Fibrolite crystals were modeled as a single cylinder whose length was determined using the experimentally determined average radius (0.2 μm) and the molar volume (200.68 cm^3/mol). Using the average E_{TW} and *A*, the excess energy due to grain boundaries was calculated to be 320 J/mol (or 300 J/mol if $b = d(110)$).

Figure 7 shows the potential shift in the andalusite-sillimanite and the kyanite-sillimanite curves for the calculated excess molar energy from the excess grain bound-

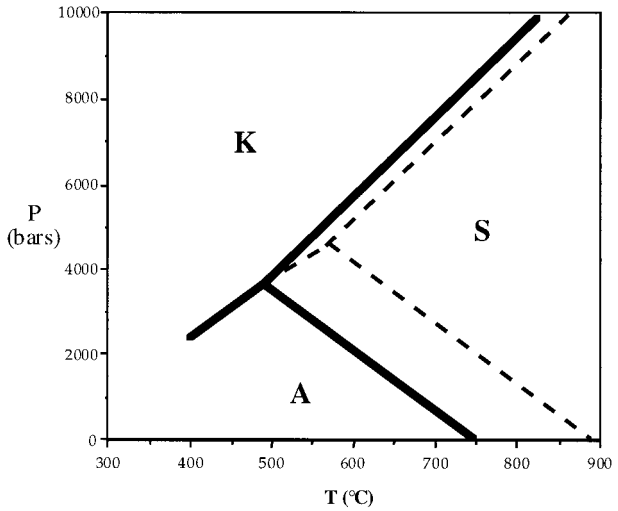

FIGURE 7. Shift of the andalusite-sillimanite and the kyanite-sillimanite phase boundaries due to the excess molar grain boundary energy of 320 J/mol as calculated for Lewiston, Idaho, fibrolite using the SDTW model (dashed lines). The solid lines represent the equilibrium phase diagram for Al_2SiO_5 calculated using data from Helgeson et al. (1978).

ary area found in fibrolite. The excess molar grain boundary energy of 320 J/mol could result in as much as a 140 °C shift of the andalusite-sillimanite equilibrium boundary and 30 °C shift of the kyanite-sillimanite equilibrium boundary.

DISCUSSION AND CONCLUSIONS

Determination of the grain boundary contribution to the total energy of fibrolite using electron diffraction and the SDTW theory results in a calculation of the aluminosilicate phase diagram where the andalusite/sillimanite boundary is potentially shifted by 140 °C and the kyanite/sillimanite boundary is shifted by 30 °C (Fig. 7). This analysis represents a minimum estimate of the excess grain boundary energy in fibrolite because SDTW theory does not account for dislocation core energies. In metals, the core energy represents 10–15% of the total (Kerrick 1990). Furthermore, the covalent nature of bonding in minerals like sillimanite likely means that the core energy of dislocations may represent >15% of the total energy (Kerrick 1990). Additional assumptions include the magnitude of the grain boundary energy contribution as independent of pressure and temperature and the angular mismatch as ''frozen in'' from a particular metamorphic event.

It is indisputable that grain boundaries contribute excess energy, but the implications for the texture development in specific metamorphic rocks are complex to predict. The result shown in Figure 7 contradicts field observations indicating fibrolite in metapelites at lower grades than coarse sillimanite (e.g., see Pattison 1992 and Kerrick 1990). This may be simply a kinetic effect that reflects larger overstepping of the phase boundary needed for nucleation of coarse-grained sillimanite or to recrystallize fibrolite to sillimanite. The higher energy of fibrolite supports the experimental results of Anderson and Kleppa (1969), Holdaway (1971), Salje (1986), and Topor et al. (1989) but contradicts the results of heat capacity comparisons performed by Hemingway et al. (1991) and several experimental studies involving the sillimanite and kyanite phase boundary by Richardson et al. (1968) and Newton (1966, 1969).

When andalusite and fibrolite coexist, the fibrolite frequently appears to be the result of a reaction between other matrix minerals rather than replacement of andalusite (Kerrick 1990). Fibrolite crystallization as long thin crystals related by low-angle tilt boundaries also suggests that fibrolite is not crystallizing from coarse-grained andalusite or kyanite. The tendency for fibrolite crystals to grow such that their *c* axes are rotated by comparatively unfavorable amounts needs to be rationalized. Because fibrolite is ubiquitously associated with micas, the explanation for both of these phenomena may be found in the nucleation process.

Previous TEM studies (e.g., Peacor 1992; Kogure and Murakami 1998; Banfield et al., unpublished data) have revealed that layer silicates are characterized by a submicrometers to a few micrometers wide crystals separated by low-angle grain boundaries. Misorientation between adjacent layer silicates is often ~10°. If fibrolite crystals replace micas during prograde metamorphism, nucleation may occur at mica grain boundaries due to the lower energy barrier compared to nucleation of an isolated crystal in the matrix. If micas were topotactically replaced by fibrolite crystals nucleated at these sites, the resulting fibrolitic mass would preserve the misorientation of the preexisting layer silicate. This may explain the relatively high-energy grain boundary structure. Some supporting evidence for topotactic relationships between layer silicates and fibrolite is found in retrograde textures reported here. However, further work is needed to determine if fibrolite crystals do in fact form by topotactic nucleation at layer silicate grain boundaries. Subsequent annealing of the resulting fibrous mass to large crystals of sillimanite would involve recrystallization, presumably requiring considerable overstepping of the phase boundary, as noted above.

Layer silicates are ubiquitous but volumetrically minor constituents of the Lewiston, Idaho, fibrolite sample (<1%). The structural and chemical characteristics suggest they are dioctahedral smectites formed by topotactic replacement during a low-temperature aqueous alteration event. It is interesting to note that the layer silicates, most of which are characterized by stacking order, are polytypically diverse and include polytypes not normally encountered in 2:1 layer silicates. From the point of view of the thermodynamic characterization of fibrolite, the existence of layer silicates is extremely important. The layer silicate crystals are too fine to allow physical separation from fibrolite, thus represent a possible source of error in calorimetric and stoichiometry studies.

Grain boundary energy may not be solely responsible for the excess energy of fibrolite in comparison to coarse-grained sillimanite. The presence of dislocations, stacking faults, Al/Si disorder, and non-stoichiometry could significantly contribute to the total energy of fibrolite. Based on dislocation density determinations and calculated strain energies, Kerrick (1986, 1990) argued that significant perturbations of the andalusite-sillimanite equilibrium boundary would require dislocation densities greater than $5 \times 10^9/cm^2$. In one fibrolite sample, analyzed by Wenk (1983), showed dislocation densities in excess of this number ($10^{10}/cm^2$). Five other samples analyzed by Gordan Nord (U.S. Geological Survey) showed average densities well below $10^8/cm^2$ (Kerrick 1986). Similarly, Doukhan et al. (1985) examined fibrolite using TEM and reported that grains were essentially dislocation free. For comparison, Doukhan et al. (1985) also examined relatively coarse-grained sillimanite crystals, with cross sections ranging from 10–100 μm, and found dislocation densities of 1 to $5 \times 10^8/cm^2$. In this study of Lewiston, Idaho, fibrolite, very low dislocation densities ($\ll 10^8/cm^2$) were observed. Furthermore, there was no evidence of stacking faults in our samples.

Zen (1969), Holdaway (1971), Greenwood (1972), and Chinner et al. (1969) suggested that fibrolite may have more Al/Si disorder than sillimanite. Unit-cell parameters increase with increasing Al/Si disorder (Beger 1979). Cell parameters were found to be virtually identical for fibrolite and sillimanite from the northeastern part of the Dalradian by Cameron and Ashworth (1972), Beger (1979), and Thomas (1984) and for Lewiston, Idaho, fibrolite (this study). However, Hemingway et al. (1991) describes results that show a difference between lattice parameters for sillimanite (Sri Lanka) and for fibrolite (Lewiston, Idaho) that corresponds to a slightly larger molar volume for fibrolite at 298.15 K and a slightly smaller molar volume for fibrolite at 1373 K (0.3% difference). Neutron diffraction showed 18% disorder in the tetrahedral sites in fibrolite from Pays de Leon, Brittany, France (Bish and Burnham 1992). These neutron diffraction data were compared to ^{29}Si nuclear magnetic resonance (NMR) data of Stebbins et al. (1993), which showed no disorder in fibrolite. To reconcile NMR data with neutron diffraction data, Stebbins et al. (1993) proposed perfect order within each Si/Al double chain but imperfect order in the relative positions of Al and Si between adjacent double chains. The contribution to configurational entropy from complete disorder between chains in a relatively equant-shaped crystal was calculated to be only 10^{-8} J/mol·K. For fibrous crystals elongated along the *c* axis with only 18% double chain disorder, the energy contribution was estimated to be even smaller (Stebbins et al. 1993). Examination of our SAED patterns revealed no evidence of streaking parallel to *a** or *b**. Based on the absence of cell parameter change and absence of evidence for disorder in diffraction patterns, we suggest no significant Si/Al disorder or short-range order in the Lewiston, Idaho, samples.

No significant differences in the non-stoichiometry of sillimanite and fibrolite have been found. However, most chemical analyses were obtained using the electron probe, which could mask 1–2 wt% variations in Al/Si ratios. Few wet chemical analyses exist, and these may be compromised by intergrown quartz and layer silicates. Assuming no significant nonstoichiometry, we conclude that the primary source of excess energy in fibrolite compared to sillimanite is grain boundary energy.

Acknowledgments

The authors thank B.L. Dutrow, L.P. Baumgartner, J.W. Valley, M. Milling, S.E. Babcock, and D. Sykes for helpful comments, with special thanks to G. Nord and B.S. Hemingway for thoughtful reviews, and acknowledge financial support from NSF grant no. EAR-950817 and a fellowship from the National Physical Science Consortium to R.L. Penn.

References cited

Anderson, P.A.M. and Kleppa, O.J. (1969) The thermochemistry of the kyanite-sillimanite equilibrium. American Journal of Science, 267, 285–290.

Bailey, S.W. (1988) X-ray diffraction identification of the polytypes of mica, serpentine, and chlorite. Clays and Clay Minerals, 36, 193–213.

Beger, R.M. (1979) Aluminum-silicon ordering in sillimanite and mullite, 312 p. Ph.D. thesis, Harvard University, Cambridge, Massachusetts.

Birch, F. (1966) Compressibility; elastic constants. In S.P. Clark Jr., Ed., Handbook of Physical Constants. Geological Society of America Memoir, 97, 97–173.

Bish, D.L. and Burnham, D.W. (1992) Rietveld refinement of the crystal structure of fibrolitic sillimanite suing neutron powder diffraction data. American Mineralogist, 77, 374–379.

Cameron, W.E. and Ashworth, J.R. (1972) Fibrolite, and its relationship to sillimanite. Nature, 235, 134–136.

Chinner, G.A., Smith, J.V., and Knowles, C.R. (1969) Transition-metal contents of Al_2SiO_5 polymorphs. American Journal of Science, 267A, 96–113.

Doukhan, J.C., Doukhan, N., Kock, P.S., and Christie, J.M. (1985) Transmission electron microscopy investigation of lattice defects in Al_2SiO_5 polymorphs and plasticity induced polymorphic transformations. Bulletin de Mineralogie, 108, 81–96.

Goldstein, A.N., Echer, C.M., and Alivisatos, A.P. (1992) Melting in semiconductor nanocrystals. Science, 256, 1425–1427.

Greenwood, H.J. (1972) Al^{iv}-Si^{iv} disorder in sillimanite and its effect on phase relations of the aluminum silicate minerals. Geological Society of America Memoir, 132, 553–571.

Gribb, A.A. and Banfield, J.F. (1997) Particle size effects on transformation kinetics and phase stability in monocrystalline TiO_2. American Mineralogist, 82, 717–728.

Helgeson, J.C., Delany, J.M., Nesbitt, H.W., and Bird, D.K. (1978) Summary and critique of the thermodynamic properties of the rock forming minerals. American Journal of Science, 278A, 229.

Hemingway, B.S., Robie, A.R., Evans, H.T. Jr., and Kerrick, D.M. (1991) Heat capacities and entropies of sillimanite, fibrolite, andalusite, kyanite, and quartz and the Al_2SiO_5 phase diagram. American Mineralogist, 76, 1597–1613.

Holdaway, M.J. (1971) Stability of andalusite and the aluminum silicate phase diagram. American Journal of Science, 271, 97–131.

Holdaway, M.J. and Mukhopadhyay, B. (1993) A reevaluation of the stability relations of andalusite: Thermochemical data and phase diagram for the aluminum silicates. American Mineralogist, 78, 298–315.

Kerrick, D.M. (1986) Dislocation strain energy in the Al_2SiO_5 polymorphs. Physics and Chemistry of Minerals, 13, 221–226.

———(1990) The Fibrolite Problem. In Mineralogical Society of America Reviews in Mineralogy, 22, 207–221.

Kogure, T. and Murakami, T. (1998) Structure and formation mechanism low-angle grain boundaries in chlorite. American Mineralogist, 87, 358–364.

Langmuir, D. and Whittemore, D.O. (1971) Variations in the Stability of Precipitated Ferric Oxyhydroxides. Advances in Chemistry Series, 106, 209–234.

McHale, J.M., Auroux, A., Perrott, A.J., and Navrotsky, A. (1997) Surface energies and thermodynamic phase stability in nanocrystalline aluminas. Science, 277, 788–791.

Newton, R.C. (1966) Kyanite-sillimanite equilibrium at 750°C. Science, 151, 1222–1225.

———(1969) Some high-pressure hydrothermal experiments on severely ground kyanite and sillimanite. American Journal of Science, 267, 278–284.

Pattison, D.R.M. (1992) Stability of andalusite and sillimanite and the Al_2SiO_5 triple point: Constraints from the Ballachulish Aureole, Scotland. Journal of Geology, 100, 423–446.

Peacor, D.R. (1992) Diagenesis and low-grade metamorphism of shales and slates. In Mineralogical Society of America Reviews in Mineralogy, 27, 335–380.

Richardson, S.W., Bell, P.M., and Gilbert, M.C. (1968) Kyanite-sillimanite equilibria: the aluminum silicate triple point. American Journal of Science, 266, 513–541.

Salje, E. (1986) Heat capacities and entropies of andalusite and sillimanite: The influence of fibrolitization on the phase diagram of the Al_2SiO_5 polymorphs. American Mineralogist, 71, 1366–1371.

Stebbins, F.F., Burnham, C.W., and Bish, D.L. (1993) Tetrahedral disorder in fibrolitic sillimanite: Comparison of ^{29}Si NMR and neutron diffraction data. American Mineralogist, 78, 461–464.

Thomas, K.K. (1984) The origin of sillimanite in Essex, Connecticut, 101 p. M.S. thesis, Indiana University, Bloomington, Indiana.

Topor, L., Kleppa, O.J., Newton, R.C., and Kerrick, D.M. (1989) Molten salt calorimetry of Al_2SiO_5 polymorphs at 1000K. Eos, 70, 493.

Vaughan, M.T. and Weidner, D.J. (1978) The relationship of elasticity and crystal structure in andalusite and sillimanite. Physical Chemistry of Minerals, 3, 133–144.

Zen, E-an (1969) The stability relations of the polymorphs of aluminum silicates: a survey and some comments. American Journal of Science, 267, 297–308.

Manuscript received September 3, 1996,
Manuscript accepted August 23, 1998
Paper handled by Gordon L. Nord Jr.